

Kinetics of the Inhibition of *Fusarium* Serine Proteinases by Barley (*Hordeum vulgare* L.) Inhibitors

ANJA I. PEKKARINEN,^{*,†,‡} COLIN LONGSTAFF,[§] AND BERNE L. JONES^{†,||,⊥}

Department of Agronomy, University of Wisconsin, Madison, Wisconsin 53706, VTT Biotechnology, 02044 VTT, Espoo, Finland, Division of Haematology, National Institute for Biological Standards and Control, Herts EN6 3QG, United Kingdom, and Cereal Crops Research Unit, Agricultural Research Service, U.S. Department of Agriculture, Madison, Wisconsin 53726

Fungal infections of barley and wheat cause devastating losses of these food crops. The endogenous proteinase inhibitors produced by plant seeds probably defend the plants from pathogens by inhibiting the degradation of their proteins by the pathogen proteases. We have studied the interactions of barley grain inhibitors with the subtilisin-like and trypsinlike proteinases of *Fusarium culmorum*. The inhibition kinetics of three inhibitor proteins, chymotrypsin/subtilisin inhibitor 2 (CI-2), barley α -amylase/subtilisin inhibitor (BASI), and Bowman–Birk trypsin inhibitor (BBBI), have been studied in detail for the first time using fungal enzymes. The kinetic studies were performed at physiological pH values to mimic in vivo conditions. Numerical approaches to kinetic analyses were used to calculate the inhibition constants, because the data analyses were complicated by some inhibitor turnover and the instability of enzymes and substrates. All were slow, tight-binding inhibitors that followed either a two-step mechanism (CI-2 and BASI) or a single-step mechanism (BBBI) under the conditions investigated. The overall K_i values derived were approximately 50 pM, 1 nM, and 0.1 nM for CI-2, BASI, and BBBI, respectively. The main difference between the CI-2 and the BASI inhibitions was accounted for by the stabilities of their final complexes and the rate constants for their second dissociation steps ($9 \times 10^{-6}/s$ and $3 \times 10^{-4}/s$, respectively). Understanding the inhibition mechanisms will be valuable in designing improved strategies for increasing the resistance of the grains to fungal infections.

KEYWORDS: Barley; *Fusarium*; proteinase; tight-binding inhibitors

INTRODUCTION

Fusarium head blight (FHB, “scab”) is a disease that is devastating to barley and wheat, and many epidemics have occurred around the world during the past century (1, 2). The fungi *Fusarium graminearum* and *Fusarium culmorum* have caused most of the epidemics, but other *Fusarium* species can also cause the disease. FHB reduces crop yields, but it causes even more losses by reducing the quality of the diseased grain so that it is unacceptable for use by the beverage, pasta, and baking industries (3, 4). It has been estimated that the infestation of wheat and barley by FHB caused direct and secondary economic losses of \$7.7 billion between 1993 and 2001 in the United States alone, where *F. graminearum* is the predominant species (5). Nearly \$1.5 billion of these losses occurred in North Dakota, South Dakota, and Minnesota, which comprise the

primary American six-row malting barley production area. The losses due to the FHB infestations caused severe stress in the farming communities and have been a major factor in the drastic decline in the malting barley production that has occurred in this area (6). The disease continues to be a serious threat because the present FHB control methods are not very effective and because it has been extremely difficult to develop resistant cultivars that have desirable agronomic and malting traits.

Fusarium species use a combination of toxins and hydrolytic enzymes to attack the wheat and barley floret tissues (7). A loss of grain storage proteins and the presence of alkaline proteinases have been associated with the FHB infections of barley and wheat (8–11), implying that the *Fusarium* proteinases, together with other hydrolytic enzymes and toxins, are strongly involved in the fungal colonization of the grains. The *Fusarium* subtilisin-like (SL) and trypsin-like (TL) proteinases used in this study have been detected in FHB-diseased barleys (12). These enzymes degraded the major barley storage protein, hordein, in vitro, and their presence in the grain was associated with the degradation of some barley albumins (12, 13).

It has been speculated that various proteinase inhibitors that are present in certain plants can defend them against some pathogens and insects by inhibiting the abilities of the invaders

* To whom correspondence should be addressed. Current address: Miller Brewing Company, 3939 W. Highland Blvd., Milwaukee, WI, 53208. Tel: 414-931-2731. Fax: 414-931-2506. E-mail: pekkarinen.anja@mbco.com.

† University of Wisconsin.

‡ VTT Biotechnology.

§ National Institute for Biological Standards and Control.

|| U.S. Department of Agriculture.

⊥ Current address: Rt. 1, Box 6, Kooskia, ID 83539.

to hydrolyze the host proteins (14, 15). Pekkarinen and Jones (16) showed that three barley chymotrypsin/subtilisin inhibitors (CI-1A, -1B, and -2) and barley α -amylase/subtilisin inhibitor (BASI) all inhibited the *F. culmorum* SL proteinase and that barley Bowman-Birk inhibitor (BBBI) inhibited its TL proteinase. All of these inhibitors were known to affect various serine proteinases, but the kinetic properties of only CI-1A, -1B, and -2 have been characterized in detail, using bacterial and mammalian enzymes (17, 18). All of these were slow, tight-binding inhibitors of bacterial subtilisins, and they bound less tightly to mammalian enzymes.

The BASI protein inhibited bacterial subtilisins strongly and some other microbial alkaline proteinases very weakly, but it did not affect either bovine chymotrypsin or trypsin (19). This inhibitor also contains a domain that inhibits the endogenous barley α -amylase II in a fast, tight-binding manner (20). BBBI inhibited mammalian trypsin and, more strongly, certain microbial TL proteinases (21). It also has a double-domain structure, which may allow it to bind two enzyme molecules simultaneously (21, 22). However, its inhibition mechanism is not known. It also weakly inhibited bovine chymotrypsin but not the *Bacillus subtilis* subtilisin or the *F. culmorum* SL proteinase (16, 21). None of the kinetic properties of the interactions of these inhibitors with fungal proteinases have been described previously.

As a part of our investigation of the roles that these inhibitors may play in plant defense mechanisms, we have studied the interactions between BBBI, chymotrypsin/subtilisin inhibitor 2 (CI-2), and BASI that were isolated from barley grain and two isolated *F. culmorum* serine proteinases. The proteinase activities were measured using small synthetic peptide substrates at pH values that were near those that occur within the grains. After our preliminary data indicated that the Michaelis-Menten kinetic analysis method was not useful for determining the inhibition constants of these inhibitions, the interactions between the enzymes and the inhibitors were studied using methods that are applicable to measuring the kinetics of slow, tight-binding inhibitions (23). The conditions used for studying the enzyme-inhibitor bindings were not optimized for kinetic studies but were chosen to reflect what occurs at the cellular pH. Because some of the enzymes and substrates were not completely stable throughout the extended analysis periods that were needed for the slow-binding inhibitor studies, these instabilities had to be accounted for in the mechanisms. We demonstrated that it is possible to carry out studies under these conditions using numerical integration approaches (24, 25).

MATERIALS AND METHODS

Enzymes. The *Fusarium* SL and TL proteinases were isolated as described previously from a culture medium in which *F. culmorum* was grown (13, 26). The enzyme concentrations were calculated from their approximate k_{cat} values (33 and 45/s for the SL and TL enzyme, respectively) by analyzing their maximal reaction velocities for hydrolyzing the synthetic substrates *N*-succinyl-Ala-Ala-Pro-Phe *p*-nitroanilide or *N*-benzoyl-Val-Gly-Arg *p*-nitroanilide. Stock solutions of the enzymes (6.0 nM SL or 1.2 nM TL proteinase) were prepared in 30 mM NH_4OAc , pH 5.0, buffer that contained 0.1 mg/mL of bovine serum albumin (BSA). The BSA, which was added to stabilize the enzymes, did not significantly affect their K_m values. The K_m values of *N*-succinyl-Ala-Ala-Pro-Phe *p*-nitroanilide for the SL proteinase and *N*-benzoyl-Val-Gly-Arg *p*-nitroanilide for the TL proteinase at pH 6.0 were 3.1 (26) and 0.11 mM (13), respectively.

Inhibitors. The inhibitors were purified from a barley (*Hordeum vulgare* L. cv. Morex) extract, and their concentrations were determined from their absorbances at 280 nm as described previously (16). Stock solutions that contained between 25 and 800 nM of inhibitor (depending on inhibitor) were prepared in water.

Kinetic Analyses. The effects of the purified inhibitors on the *F. culmorum* enzyme activities were measured both with and without preincubation of the enzyme (E) and the inhibitor (I) in order to study the association kinetics of E and I and the dissociation of the EI complexes, as described by Williams and Morrison (27). To study the association of E and I, the inhibitors were mixed with the substrate (S) solutions and preincubated at 28 °C for 15 min. The enzymes were preincubated without inhibitors at 28 °C for 30 min. The reactions were started by adding 5 μL of the enzyme solutions to 95 μL aliquots of the preincubated S + I mixtures. To study the dissociation of the preformed EI complexes, the enzyme solutions were preincubated with each inhibitor (or without the inhibitor for measuring the uninhibited reactions) at 28 °C for 30 min. The reactions were started by mixing 5 μL of the preincubated E + I mixtures with 95 μL aliquots of the substrate solution that had been incubated at 28 °C for 15 min. Similar reaction mixtures were prepared with water in place of the inhibitor solution to measure the uninhibited enzyme activities. The final reaction concentrations of the SL and TL proteinases were 150 and 30 pM, respectively. The inhibitor concentrations were 3.75, 5.0, 7.5, and 10 nM for CI-2; 2.5, 5.0, 10, and 20 nM for BASI; and 1.25, 2.5, and 5.0 nM for BBBI. The final substrate concentrations were 7.0 mM *N*-succinyl-Ala-Ala-Pro-Phe *p*-nitroanilide (SL activities) or 1.0 mM *N*-benzoyl-Val-Gly-Arg *p*-nitroanilide (TL activities) in a solution of 4% dimethyl sulfoxide and 170 mM sodium citrate, pH 6.0. The substrates were purchased from Sigma (St. Louis, MO).

Eighty microliters of each reaction mixture was transferred into one of the cells of an eight cell holder, whose top was then sealed with Parafilm to prevent evaporation. The time between the mixing of the uninhibited reaction and the start of taking the absorbance readings was 6 min. The absorbances of the reaction mixtures were monitored at 405 nm with a temperature-controlled cuvette in a Shimadzu BioSpec-1601 spectrophotometer at 28 °C for at least 16 h. The absorbances of the reaction mixtures were read once every minute for 1 h, then every 3 min for 3 h, and finally every 15 min for 15 h. Appropriate substrate controls without enzymes were analyzed under the same conditions.

Data Analyses. The general pattern of analysis was initially to use classical (analytical) slow-binding inhibition approaches to determine initial and final K_i values and rate constants for slow-binding steps wherever possible. This was done using nonlinear curve fitting of the raw data using Grafit (24) and eq 1, which is appropriate for reactions that proceed to equilibrium between E and I in the presence of a chromogenic substrate (28).

$$\text{absorbance} = A_0 + v_s t + (v_0 - v_s) [1 - \exp(-k_{\text{obs}} t)] / k_{\text{obs}} \quad (1)$$

where A_0 is the initial absorbance at time zero, v_0 is the initial rate, v_s is the final rate at equilibrium, and k_{obs} is the apparent first-order rate constant for the development of the steady state between the free E, I, and EI complex.

Further analyses were performed using the DynaFit program, in which curve fitting is done by numerical integration (25). These made it possible to analyze complex mechanisms that could account for the enzyme and substrate instabilities and inhibitor turnover, which was not possible using traditional analytical approaches. Using the numerical approach, the reactions taking place in the system are described in a script file using a standard notation, and initial estimates for rate constants and concentrations are given. The program simulates the system and provides the best estimates by iteration for rate constants that are identified as variables to be fitted.

RESULTS AND DISCUSSION

CI-2. Curve fitting via analytical approaches and nonlinear regression fitting using Grafit was successful and produced results that fit the observed reaction curves well (Figure 1). A reasonable estimate of $2.6 \times 10^5 \text{ M/s}$ for the association rate constant was obtained from the plot of the observed rate constant (k_{obs}) vs inhibitor concentration $[I]$ (not shown). A hyperbolic curvature of the plot would have indicated that it was a two-step reaction, but because of the limited working range of $[I]$, such curvature was difficult to confirm. However, the curve

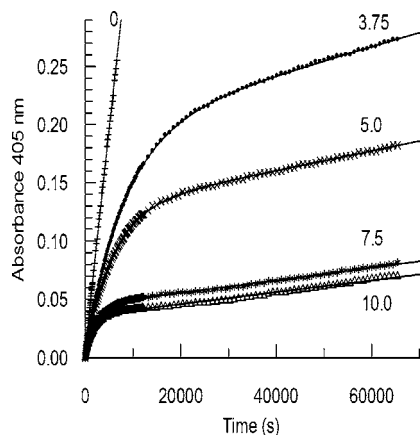


Figure 1. Slow-binding inhibition of the SL *Fusarium* proteinase by the barley CI-2 inhibitor. The symbols indicate measured absorbances, and the solid lines are the results obtained from curve fitting.

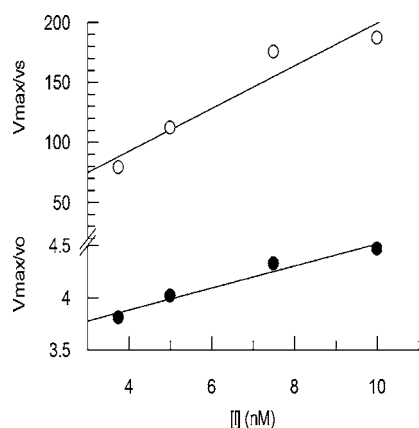


Figure 2. Plots of V_{\max}/v_s and V_{\max}/v_0 derived from values fitted to the data of **Figure 1**. The slopes of these lines were used to calculate K_{ii} (9.5 nM) and K_{if} (56 pM): the initial K_i for complex formation (closed symbols) and the overall reaction K_i (open symbols), respectively.

fitting results showed that the calculated initial reaction rates (v_0) decreased with increasing $[I]$ (**Figure 1**), a phenomenon that is indicative of the two-step reaction that is depicted in eq 2 (23):



The rate constant, k_4 , value of $9.5 \times 10^{-6}/s$ for the dissociation of the EI' complex was calculated from the initial and steady-state reaction rates (v_0 and v_s) and k_{obs} of the curves in **Figure 1**. However, this value may not be completely accurate, as there was some systematic deviation of k_4 with increasing $[I]$. The changes in the fitted values of v_0 and v_s with various $[I]$ were further analyzed using Grafit to estimate the initial and final inhibition constants (K_{ii} and K_{if}) of the EI complex formation (**Figure 2**). A K_{ii} value of 9.5 nM was obtained for the initial loose complex EI , and a K_{if} of 56 pM was obtained for the final tight complex EI' . An average value of $1.0 \times 10^{-5}/s$ for k_4 was derived from eq 3 (29, 30):

$$k_{\text{obs}} = k_4[(1 + I/\text{app}K_{if})/(1 + I/\text{app}K_{ii})] \quad (3)$$

and an estimated value of $1.6 \times 10^{-3}/s$ for k_3 was obtained from eq 4:

$$k_3 = (K_{ii}k_4/K_{if}) - k_4 \quad (4)$$

Table 1. Comparison of the Constants for the Binding of CI-2 to SL Proteinase as Determined Using Grafit and DynaFit Analyses

parameter	Grafit ^a	DynaFit (estimated error %)
K_{ii} (nM)	9.5	6.9 (1.5)
K_{if} (pM)	56	45 ^b (<5)
k_3 ($\times 10^{-3}/s$)	1.6	1.4 (0.6)
k_4 ($\times 10^{-6}/s$)	9.5	8.8 (4.7)

^a Curve fittings for linear and nonlinear regression generally have a standard error of 15–20%. The values were corrected for the effects of substrate when necessary; for example, $K_{ii} = \text{app}K_{ii}/(1 + S/K_m)$. ^b Calculated from $K_{ii} \times k_4/(k_3 + k_4)$.

Further analyses of the CI-2 binding were performed using numerical integration and the program DynaFit. Up to a 20% error in the estimation of the CI-2 concentration was also permitted when applying DynaFit, as is recommended. As shown in **Table 1**, the results obtained with the Grafit analytical approach and DynaFit numerical approach were in good agreement.

The dissociation of preformed complexes was also investigated using numerical analysis. However, it was not possible to use the data from the preincubation experiments to determine the inhibition constants, because the final results for k_3 and k_4 were dependent on the initial values provided for k_1 and k_2 , which cannot be determined directly by these dissociation experiments.

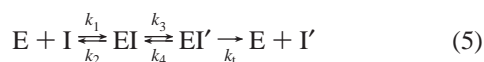
Previous studies have shown that CI-2 is a slow, tight-binding inhibitor of bacterial subtilisin BPN' (18). As opposed to the two-step interaction between the SL proteinase and the CI-2 observed in this study, the inhibition of the subtilisin BPN' followed a simple $E + I \leftrightarrow EI$ model with a K_i (analogous to K_{if} in our nomenclature) value of 2.9 pM. The K_{if} value of 45 pM (**Table 1**) implies that the CI-2 interacted less strongly with the *Fusarium* SL proteinase than with the bacterial subtilisin. The same substrate was used in both studies, but the analyses were performed at different pH values, which may account for the differences found in both the reaction models and the inhibition constant values. In this study, the reactions were not carried out at the optimal pH (approximately 9) for the SL proteinase activity, but at pH 6, which is approximately the pH of ground barley grain that is suspended in water.

It has been suggested that inhibitors show tight binding when their total enzyme concentration to inhibition constant (E_t/K_i) ratios are greater than 0.1 (23). According to this criterion, CI-2 is a tight-binding inhibitor of the SL proteinase. CI-2 has a Met⁵⁹-Glu⁶⁰ reactive site bond that subtilisin should normally cleave, and the question of why CI-2 acts as an inhibitor instead of a substrate has intrigued researchers for decades. The inhibition behavior can be partially accounted for by substrate specificity, as the mutation of Met⁵⁹ to Lys⁵⁹ increased the susceptibility of CI-2 to hydrolysis by subtilisin BPN' (18). In addition, Longstaff et al. (18) proposed that the formation of a rigid inhibitor structure with a stabilized binding loop could explain the resistance of inhibitors to cleavage. Alternatively, the inhibited species was an acyl-enzyme complex that favored religation of the cleavage bond. Radisky and Koshland (31) suggested that CI-2 and subtilisin BPN' form a stable acyl-enzyme intermediate that can very slowly dissociate to yield cleaved CI-2 and active enzyme. They further showed that the C-terminal Gly⁸³ and the β -sheet structure in the binding loop of CI-2 were critical for stabilizing its hydrogen-bonding network, which, in turn, inhibited the deacylation of the intermediate (32). Similar interactions can occur between the SL proteinase and the CI-2. Even though the turnover of CI-2

was not observed in this study, it is possible that the hydrolysis occurred at a very slow rate.

BASI. It initially appeared that the inhibition of the SL proteinase by BASI showed some slow-binding behavior but that the complex was not as tight binding as the SL proteinase–CI-2 complex. The observed decrease in the v_o (**Figure 3A**) with increasing [I] indicated that this was a two-step inhibition mechanism. However, careful inspection of the data showed that there was an initial inhibition that was followed by a partial recovery of activity (**Figure 3B**), which could have been due to a turnover of inhibitor. To diminish the impact of this possible inhibitor turnover on the inhibition results, a traditional Grafit analysis for slow-binding kinetics was performed using data from only the first 6000 s of reaction, during which the turnover was less significant.

Data fitting using the first 6000 s of data was reasonably successful (**Figure 3A**), and the decrease in the v_o with increasing [I] was still apparent, indicating that a two-step mechanism was involved. Indications of the possible turnover of inhibitor can be seen in the representative curves shown in **Figure 3B**, where the fitted curves obtained for the data from the first 6000 s are overlaid on the data obtained throughout the entire 60000 s experiment. The two curves carried out with the highest [I], where fitting is more reliable during the early parts of the experiment, show that there is a gradual increase in the enzymatic activities, which is consistent with the inhibitor undergoing hydrolysis. Hence, the mechanism proposed for this system is



where EI is the initial complex of SL proteinase and BASI, EI' is the complex that leads to the hydrolysis of BASI, the I' is cleaved and inactive BASI, and k_t is the rate constant for the turnover of EI'.

The starting estimates of the initial K_i and overall K_i values (K_{ii} and K_{if} , for the formation of EI and EI', respectively) and rate constants k_3 and k_4 were derived from the fittings of the data that were collected during the first 6000 s. The values were calculated using two independent sets of BASI data, in the same way that the CI-2 values were calculated above. DynaFit was then used to calculate the inhibition constants for the two-step inhibition model with and without the turnover of I. All of the BASI data from both 60000 s data sets were included. All methods gave broadly similar results (**Table 2**). Curve fitting of the data that was collected for only the first 6000 s did not yield DynaFit results that differed significantly from the 60000 s results (not shown). Both values of K_{ii} and K_{if} were of the same magnitude, although the K_{if} was roughly five times lower than K_{ii} . The final model, which includes the inhibitor turnover, does show a small improvement in the sum of squares (1.2×10^{-4}) for the curve fitting using DynaFit, as compared to the model without inhibitor turnover (1.4×10^{-4}). This is not a dramatic improvement, but it demonstrates that this type of mechanism is amenable to analysis using this approach. It would be even more critical to be able to calculate this in cases where the inhibitor turned over more quickly.

The lower binding affinity and higher hydrolysis rate of BASI make it a less potent inhibitor than CI-2. This was largely accounted for by the difference in the k_4 value, as is often observed. In addition, the barley α -amylase II enzyme activity may interfere with the binding of the SL proteinase to BASI in the grain. The overall K_i of BASI for α -amylase II at pH 8 was 22 pM (20), which implies that BASI may bind more tightly to the α -amylase than to the SL proteinase. However, the effects of α -amylase II on the inhibition were not determined in this

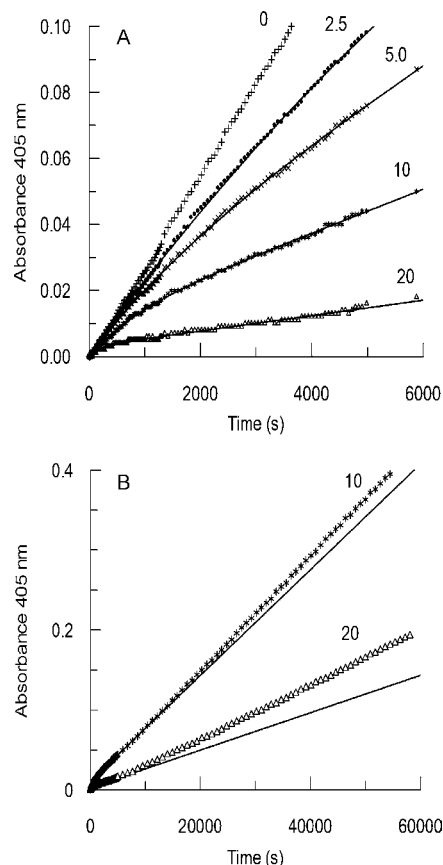


Figure 3. Slow-binding inhibition curves for BASI with the *Fusarium* SL proteinase. The symbols indicate measured absorbances, and the solid lines are the results obtained from curve fitting. (A) The first 6000 s of the data. (B) The total 60000 s of the data with 10 and 20 nM BASI. The recovery of enzymatic activity with time indicates that the inhibitor is being hydrolyzed.

Table 2. Inhibition Constants and Rates of Formation for the SL Proteinase–BASI System Calculated Using Different Analysis Methods^a

parameter	A	B	C
K_{ii} (nM)	4.8	5.7	4.5
K_{if} (nM)	1.0	1.4	0.8
k_3 ($\times 10^{-3}$ /s)	1.2	1.2	1.4
k_4 ($\times 10^{-3}$ /s)	0.3	0.4	0.3
k_t ($\times 10^{-3}$ /s)	NA	NA	0.2

^a A, Grafit analysis using the first 6000 s of the reaction data; B, DynaFit analysis for two-step inhibition model using all of the 60000 s reaction data; and C, DynaFit analysis similar to B but with a term for inhibitor turnover included. NA, not applicable.

study and the effect of pH on the relative bindings of the two enzymes is not known.

As with BASI, turnover of the CI-1A inhibitor may have complicated the analysis of its activity. CI-2 and CI-1 are similar proteins, but the latter is generally a weaker inhibitor of the various serine proteinases (16, 17). Neither the traditional Michaelis–Menten analysis nor the slow-binding inhibitor analysis method could be successfully applied to determining the K_i for the inhibition of the SL proteinase by CI-1A (data not shown). However, the collected data suggested that the inhibition by CI-1A was slower and its binding was even less tight than they were with BASI (data not shown).

BBBI. The BBBI inhibition analysis was carried out using both the uncorrected raw data and the same data after it was corrected to account for the significant levels of substrate

Table 3. Calculated Kinetic Constants for the Inhibition of the TL Proteinase by BBBI^a

parameter	A			B		C	
	Gra 1	Dyn 1	Dyn 2	Dyn 1	Dyn 2	Dyn 1	Dyn 2
k_{on} ($\times 10^5$ /M/s)	4.1	2.2	2.8	2.9	2.9	2.7	2.7
k_{off} ($\times 10^{-5}$ /s)	1.9	1.3	2.7	2.3	3.0	2.5	2.0
K_i (pM)	46	58	94	82	103	91	74

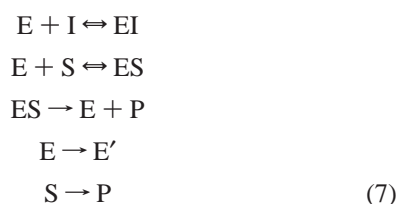
^a The constants were calculated from formation (Gra1 or Dyn1) and dissociation (Dyn2) experiments using A, corrected data (substrate autolysis subtracted); B, uncorrected data with a term for substrate autolysis; or C, uncorrected data with terms for both substrate autolysis and loss of enzyme included. The data were analyzed by Grafit (Gra) and DynaFit (Dyn).

autolysis. The initial analysis was performed on corrected data (substrate autolysis subtracted) using both Grafit and DynaFit. The uncorrected data were analyzed using DynaFit, and the analysis included a term that accounted for the background hydrolysis of substrate, in the absence of added proteinase. Examination of the data revealed a further complication when it was observed that enzyme activity was lost in the absence of inhibitor, suggesting enzyme instability. The data and preliminary analyses both strongly indicated that these phenomena occurred. The rate constants for both the substrate hydrolysis in the absence of enzyme ($k_{sh} = 7.0 \times 10^{-8}$ /s) and the enzyme inactivation ($k_{ei} = 6.8 \times 10^{-5}$ /s) were derived from the data by curve fitting using DynaFit on data obtained in the absence of inhibitor. Data for the dissociation of preformed EI complex were also analyzed using DynaFit, using both corrected and uncorrected data.

Over the narrow range of [I] that was used in this experiment, there was no variation in the v_o with increasing [I] and the k_{obs} vs [I] plot was linear. These findings imply that, under the conditions used, the inhibition of the TL proteinase by BBBI occurred via a single-step process that can be described as in eq 6:



The data analyses provided values for K_i and two rate constants, k_{on} and k_{off} (Table 3). In the Grafit analysis, K_i was calculated from v_o and v_s , the k_{on} was calculated from the k_{obs} that was derived from curve fitting, and k_2 was calculated from $k_{off} = K_i \times k_{on}$. With DynaFit, the k_{on} and k_{off} values were determined from numerical integration and K_i was calculated from the relationship $K_i = k_{off}/k_{on}$. Taking the unstable substrate and enzyme into account, the model used for numerical integration with DynaFit was



where E' is inactive enzyme and P is the product of the substrate (S) hydrolysis.

Using DynaFit, the curve fittings gave good results when both corrected and uncorrected data were analyzed, but the best fittings were obtained with data that had been corrected for both substrate autolysis and enzyme inactivation (Figure 4). The improvement in the fittings over those obtained with the uncorrected data can be seen in the residual plots (Figure 5). Also, the sum of the squares for the fittings improved from 5.3

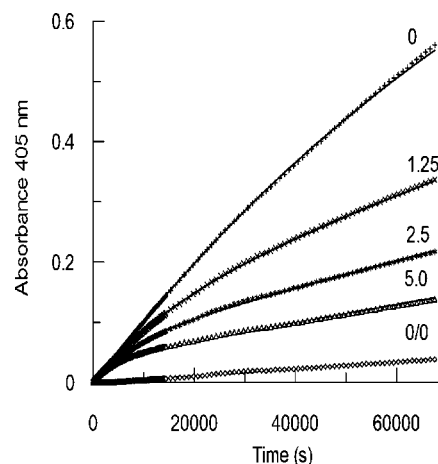


Figure 4. Inhibition curves obtained when the TL proteinase was inhibited by BBBI. The inhibitor concentrations in nanomolar are indicated; the proteinase concentration was 30 pM. The reaction marked 0/0 contained neither inhibitor nor enzyme. The symbols indicate measured data, and the solid lines show the fitting of the data that resulted from applying DynaFit analysis and eq 7.

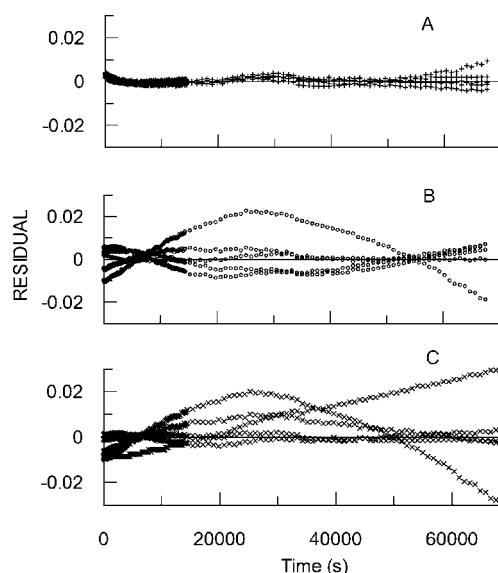


Figure 5. Residual plots showing the differences between the observed data and the curves from data fitted using DynaFit. (A) Data fitted to eq 7, which resulted in the smallest sum of squares (2.2×10^{-6}). (B) Data fitted to a model including the term for unstable substrate but without any term for unstable enzyme (sum of squares = 3.1×10^{-5}). (C) Data fitted to a model without unstable enzyme or background substrate hydrolysis (sum of squares = 5.3×10^{-5}).

$\times 10^{-5}$ (no unstable enzyme or substrate correction) to 3.1×10^{-5} (corrected for unstable enzyme) to 2.2×10^{-6} (corrected for both enzyme and substrate). A further marginal improvement in the sum of squares for fitting was obtained if a term for the inactivation of the ES complex was also included in the eq 7 model. However, these improvements may not be significant and may simply arise from adding additional parameters to the analysis, rather than because the model is more realistic.

The dissociation of preformed complexes was also examined, and similar kinetic constants were obtained (Table 3). This was irrespective of the fitting approach that was used. The curve fitting to the data from the dissociation of preformed complexes was improved when a term was included for the enzyme instability (data not shown). Inclusion of this term did not affect the rate constants k_{on} and k_{off} very much (Table 3). However,

the sum of squares for the fittings was improved markedly by fitting to the data without inhibitor, whereby the sum of squares was reduced from 2.6×10^{-5} to 5.3×10^{-7} .

The BBBI molecule comprises two very similar domains, and it has been shown using X-ray crystallography that BBBI should be able to bind two trypsin molecules simultaneously (22). However, because of differences in the amino acids at the active sites of its two domains, trypsin and TL proteinases would probably not bind to both domains with the same affinity. Boisen and Djurtoft (21) calculated that during their investigation BBBI bound two trypsin molecules simultaneously, but during this study, no evidence of such two-enzyme binding was observed and simple enzyme inhibitor binding models adequately explained the results observed.

Inhibitor–Enzyme Interactions in the Grain. The efficacy of these barley inhibitor proteins for inhibiting the pathogen proteinases *in vivo* depends on the relative concentrations of the inhibitors and the proteinases at the infection site. The purification of the BASI, CI-2, and BBBI from the barley cv. Morex yielded 35, 18, and 13 mg/kg of grain, respectively, but portions of the inhibitors had probably been lost during purification (16). Other studies have shown that the BASI concentrations in the mature grains of various barley cultivars varied between 50 and 450 mg/kg of grain (33–35). Boisen and Djurtoft (21) estimated that the BBBI content of the barley cv. Bomi was roughly 100 mg/kg of grain. Estimates of the free SL and TL proteinase concentrations of diseased barley, calculated from the enzyme activities of their extracts (12), were 10 and 1 mg/kg of grain, respectively. However, because the CI-2, BASI, and BBBI inhibitors readily bind to the proteinases, it is likely that the total enzyme concentrations of the diseased grain were greater than calculated because the activities were probably partially suppressed by their inhibitors. The total proteinase inhibition would also depend on the relative affinities of the proteinases for the various protein substrates that were present and the affinities of the various inhibitors for other enzymes such as barley α -amylase II or, possibly, some endogenous proteinases. These values for the rate and equilibrium constants and concentrations of the enzymes and inhibitors make it possible to simulate the kinetics of their interactions and to estimate the levels of the free and bound enzyme and inhibitor populations in grain. Because we determined the rate constants under physiological conditions, rather than under the idealized conditions that are often used for enzyme mechanistic studies, our results can be used to clarify the behavior of the enzymes and their inhibitors *in vivo*.

Grain plants are most susceptible to the *Fusarium* during anthesis, when the fungus has a direct access to the inner part of the flower, and they remain relatively susceptible during the first few weeks of the development of the kernel (7). The interaction between the floret and the fungus is probably biotrophic during the beginning of the infection (7). During this time, the *F. culmorum* proteinases may suppress some defense reactions of the plants by degrading the barley pathogenesis-related (PR) proteins in the same way that a SL proteinase from *F. solani* f. sp. *eumartii* degraded potato PR proteins (36). Whether or not the SL or TL proteinases are active in barley grains during the early stages of infection has not been shown, but gene expression of some TL and SL proteinases as well as other proteinases has been detected in *Fusarium*-infected barley plants within 6 days of inoculation (37).

The endogenous proteinase inhibitors can probably retard the colonization of the seed by the fungi, because one or the other of the inhibitors is expressed in various tissues. However, they are probably not present immediately after anthesis. The synthesis of CI-2 and BASI has been detected approximately 2

weeks after anthesis (38, 39). BASI is present in the starchy endosperm and embryo (39), and CI-2 has been demonstrated to occur in the aleurone layer and starchy endosperm, but not in the embryo, of the mature grain (40). BBBI has been detected in barley embryos and aleurone layers but not in its starchy endosperm (21). The time during which BBBI is synthesized in the developing kernel has not been determined, but BBBI is present in the rootlets of germinating barley (41). None of the three inhibitors has been detected in the outer layers (husk, pericarp, or testa) of the kernel. As our study shows that the inhibitors, especially CI-2 and BBBI, can effectively bind the *Fusarium* proteinases, it may be possible to enhance the resistance of barley against *Fusarium* using genetic engineering to target the expression of one or two of these inhibitors to the outer layers of the kernel. Developing such barley line(s) could be useful in investigating the role of proteinases at the early stages of *Fusarium* infection.

In summary, this study has shown that CI-2 and BBBI inhibited the *Fusarium* SL and TL proteinases, respectively, in a slow, tight-binding manner. The inhibition of the SL proteinase by BASI was borderline tight-binding, with a slow hydrolysis of the inhibitor occurring under the assay conditions. Overall, the results indicate that the data analysis methods employed were valid and the use of numerical simulation and curve fitting (using DynaFit) allowed us to develop models for the enzyme–inhibitor interactions. Some of these interaction models were rather elaborate and included terms for the turnover of the inhibitors and the instabilities of the enzymes and substrates. These models were critical for correctly determining the rate constants as these interactions made it impossible to use the traditional enzyme inhibition analytical methods. The numerical approaches will be even more helpful when studying systems in which the inhibitor turnover is even greater than that observed here. Even those inhibitors that are poor substrates may nevertheless be important enzyme activity regulators *in vivo* and need to be studied.

ABBREVIATIONS USED

BASI, barley α -amylase/subtilisin inhibitor; BBBI, barley Bowman–Birk inhibitor; BSA, bovine serum albumin; CI-2, chymotrypsin/subtilisin inhibitor 2; SL, subtilisin-like; TL, trypsinlike.

LITERATURE CITED

- (1) Parry, D. W.; Jenkinson, P.; McLeod, L. *Fusarium* ear blight (scab) in small grain cereals—A review. *Plant Pathol.* **1995**, *44*, 207–238.
- (2) Steffenson, B. J. *Fusarium* head blight of barley: Impact, epidemics, management, and strategies for identifying and utilizing genetic resistance. In *Fusarium Head Blight of Wheat and Barley*; Leonard, K. J., Bushnell, W. R., Eds.; American Phytopathological Society Press: St. Paul, MN, 2003; pp 241–295.
- (3) Schwarz, P. B. Impact of *Fusarium* head blight on malting and brewing quality of barley. In *Fusarium Head Blight of Wheat and Barley*; Leonard, K. J., Bushnell, W. R., Eds.; American Phytopathological Society Press: St. Paul, MN, 2003; pp 395–419.
- (4) Dexter, J. E.; Nowicki, T. W. Safety assurance and quality assurance issues associated with *Fusarium* head blight in wheat. In *Fusarium Head Blight of Wheat and Barley*; Leonard, K. J., Bushnell, W. R., Eds.; American Phytopathological Society Press: St. Paul, MN, 2003; pp 420–460.
- (5) Nganje, W. E.; Kaitibie, S.; Wilson, W. W.; Leistriz, F. L.; Bangsund, D. A. *Economic Impacts of Fusarium Head Blight in Wheat and Barley: 1993–2001*; Agribusiness and Applied Economics Report No. 538; North Dakota State University: Fargo, ND, 2004.

- (6) McMullen, M. Impacts of *Fusarium* head blight on the North American agricultural community: The power of one disease to catapult change. In *Fusarium Head Blight of Wheat and Barley*; Leonard, K. J., Bushnell, W. R., Eds.; American Phytopathological Society Press: St. Paul, MN, 2003; pp 484–503.
- (7) Bushnell, W. R.; Hazen, B. E.; Pritsch, C. Histology and physiology of *Fusarium* head blight. In *Fusarium Head Blight of Wheat and Barley*; Leonard, K. J., Bushnell, W. R., Eds.; American Phytopathological Society Press: St. Paul, MN, 2003; pp 44–83.
- (8) Bechtel, D. B.; Kaleikau, L. A.; Gaines, R. L.; Seitz, L. M. The effects of *Fusarium graminearum* infection on wheat kernels. *Cereal Chem.* **1985**, *62*, 191–197.
- (9) Nightingale, M. J.; Marchylo, B. A.; Clear, R. M.; Dexter, J. E.; Preston, K. R. *Fusarium* head blight: Effect of fungal proteases on wheat storage proteins. *Cereal Chem.* **1999**, *76*, 150–158.
- (10) Jackowiak, H.; Packa, D.; Wiwart, M.; Perkowski, J.; Buško, M.; Borusiewicz, A. Scanning electron microscopy of mature wheat kernels infected with *Fusarium culmorum*. *J. Appl. Genet.* **2002**, *43A*, 167–176.
- (11) Schwarz, P. B.; Jones, B. L.; Steffenson, B. J. Enzymes associated with *Fusarium* infection of barley. *J. Am. Soc. Brew. Chem.* **2002**, *60*, 130–134.
- (12) Pekkarinen, A. I.; Sarlin, T. H.; Laitila, A. T.; Haikara, A. I.; Jones, B. L. *Fusarium* species synthesize alkaline proteinases in infested barley. *J. Cereal Sci.* **2003**, *37*, 349–356.
- (13) Pekkarinen, A. I.; Jones, B. L. Trypsin-like proteinase produced by *Fusarium culmorum* grown on grain proteins. *J. Agric. Food Chem.* **2002**, *50*, 3849–3855.
- (14) Boisen, S. Protease inhibitors in cereals. Occurrence, properties, physiological role and nutritional influence. *Acta Agric. Scand.* **1983**, *33*, 369–381.
- (15) Ryan, C. A. Protease inhibitors in plants: Genes for improving defenses against insects and pathogens. *Annu. Rev. Phytopathol.* **1990**, *28*, 425–449.
- (16) Pekkarinen, A. I.; Jones, B. L. Purification and identification of barley (*Hordeum vulgare* L.) proteins that inhibit the alkaline serine proteinases of *Fusarium culmorum*. *J. Agric. Food Chem.* **2003**, *51*, 1710–1717.
- (17) Greagg, M. A.; Brauer, A. B. E.; Leatherbarrow, R. J. Expression and kinetic characterization of barley chymotrypsin inhibitors 1a and 1b. *Biochim. Biophys. Acta* **1994**, *1222*, 179–186.
- (18) Longstaff, C.; Campbell, A. F.; Fersht, A. R. Recombinant chymotrypsin inhibitor 2: Expression, kinetic analysis of inhibition with α -chymotrypsin and wild-type and mutant subtilisin BPN', and protein engineering to investigate inhibitory specificity and mechanism. *Biochemistry* **1990**, *29*, 7339–7347.
- (19) Yoshikawa, M.; Iwasaki, T.; Fujii, M.; Oogaki, M. Isolation and some properties of a subtilisin inhibitor from barley. *J. Biochem.* **1976**, *79*, 765–773.
- (20) Sidenius, U.; Olsen, K.; Svensson, B.; Christensen, U. Stopped-flow kinetic studies of the reaction of barley α -amylase/subtilisin inhibitor and the high pI barley α -amylase. *FEBS Lett.* **1995**, *361*, 250–254.
- (21) Boisen, S.; Djurtoft, R. Protease inhibitor from barley embryo inhibiting trypsin and trypsin-like microbial proteases. Purification and characterization of two isoforms. *J. Sci. Food Agric.* **1982**, *33*, 431–440.
- (22) Song, H. K.; Kim, Y. S.; Yang, J. K.; Moon, J.; Lee, J. Y.; Suh, S. W. Crystal structure of a 16 kDa double-headed Bowman-Birk trypsin inhibitor from barley seeds at 1.9 Å resolution. *J. Mol. Biol.* **1999**, *293*, 1133–1144.
- (23) Szedlacsek, S. E.; Duggleby, R. G. Kinetics of slow and tight-binding inhibitors. *Methods Enzymol.* **1995**, *249*, 144–180.
- (24) Leatherbarrow, J. *Grafit*, version 5; Erithacus Software: Staines, United Kingdom, 1988.
- (25) Kuzmič, P. Program DYNAFIT for the analysis of enzyme kinetic data: Application to HIV proteinase. *Anal. Biochem.* **1996**, *237*, 260–273.
- (26) Pekkarinen, A. I.; Jones, B. L.; Niku-Paavola, M.-L. Purification and properties of an alkaline proteinase of *Fusarium culmorum*. *Eur. J. Biochem.* **2002**, *269*, 798–807.
- (27) Williams, J. W.; Morrison, J. F. The kinetics of reversible tight-binding inhibition. *Methods Enzymol.* **1979**, *63*, 437–467.
- (28) Longstaff, C. In vivo significance of kinetic constants of tight binding reversible proteinase inhibitors. *Thromb. Haemostasis* **1992**, *67*, 533–536.
- (29) Longstaff, C.; Gaffney, P. J. Serpin-serine protease binding kinetics: α 2-antiplasmin as a model inhibitor. *Biochemistry* **1991**, *30*, 979–986.
- (30) Longstaff, C.; Gaffney, P. J. Studies on the mechanism of binding of serpins and serine proteases. *Blood Coag. Fibrinol.* **1992**, *3*, 89–97.
- (31) Radisky, E. S.; Koshland, D. E., Jr. A clogged gutter mechanism for protease inhibitors. *Proc. Natl. Acad. Sci. U.S.A.* **2002**, *99*, 10316–10321.
- (32) Radisky, E. S.; King, D. S.; Kwan, G.; Koshland, D. E., Jr. The role of the protein core in the inhibitory power of the classic serine protease inhibitor, chymotrypsin inhibitor 2. *Biochemistry* **2003**, *42*, 6484–6492.
- (33) Munck, L.; Mundy, J.; Vaag, P. Characterization of enzyme inhibitors in barley and their tentative role in malting and brewing. *J. Am. Soc. Brew. Chem.* **1985**, *43*, 35–38.
- (34) Masojc, P.; Zawistowski, J.; Zawistowska, U.; Howes, N. K. A combined monoclonal and polyclonal antibody sandwich ELISA for quantification of the endogenous α -amylase inhibitor in barley and wheat. *J. Cereal Sci.* **1993**, *17*, 115–124.
- (35) Jarrett, S. J.; Marschke, R. J.; Symons, M. H.; Gibson, C. E.; Henry, R. J.; Fox, G. P. Alpha-amylase/subtilisin inhibitor levels in Australian barleys. *J. Cereal Sci.* **1997**, *25*, 261–266.
- (36) Olivieri, F.; Zanetti, M. E.; Oliva, C. R.; Covarrubias, A. A.; Casalougué, C. A. Characterization of an extracellular serine protease of *Fusarium eumartii* and its action on pathogenesis related proteins. *Eur. J. Plant Pathol.* **2002**, *108*, 63–72.
- (37) Güldener, U.; Seong, K.-Y.; Boddu, J.; Cho, S.; Trail, F.; Xu, J.-R.; Adam, G.; Mewes, H.-W.; Muehlbauer, G. J.; Kistler, H. C. Development of a *Fusarium graminearum* Affymetrix Gene-Chip for profiling fungal gene expression in vitro and in planta. *Fungal Genet. Biol.* **2006**, *43*, 316–325.
- (38) Rasmussen, U.; Williamson, M. S.; Mundy, J.; Kreis, M. Differential effects of the Hiproly Lys1 gene on the developmental synthesis of (lysine-rich) proteins from barley endosperm. *Plant Sci.* **1988**, *55*, 255–266.
- (39) Hill, R. D.; Gubbels, S. M.; Boros, L.; Sumner, M. J.; MacGregor, A. W. Location of α -amylase/subtilisin inhibitor during kernel development and germination. *Can. J. Bot.* **1995**, *73*, 982–990.
- (40) Rasmussen, U. Immunological screening for specific protein content in barley seeds. *Carlsberg Res. Commun.* **1985**, *50*, 83–93.
- (41) Nagasue, A.; Fukamachi, H.; Ikenaga, H.; Funatsu, G. The amino acid sequence of barley rootlet trypsin inhibitor. *Agric. Biol. Chem.* **1988**, *52*, 1505–1514.

Received for review November 3, 2006. Revised manuscript received January 24, 2007. Accepted January 25, 2007. The financial support of the American Malting Barley Association and Miller Brewing Co. are greatly appreciated.

JF0631777